ARTICLE OPEN

Check for updates

Compressive strength degradation of engineered bamboo subjected to fungal attack

C. Q. Chen[1,2], S. J. Zhang[2], Y. B. H. Kong[2], T. Ji[3,4], W. W. Huang[4,5,6], Y. T. Hu[7], D. W. Zhang[7,8,9] and Y. Xiao[10,11]✉

Glue laminated bamboo (glubam) is a type of engineered bamboo material developed for applications in building structures and interiors. This paper focuses on the fungal (*Aspergillus niger*) colonization from 14 to 56 days in thick- and thin-strip glubam board with the investigation of physical, mechanical (compression), and microcosmic properties. Two-degree of carbonization treatment was employed to improve the antifungal property of the thick-strip glubam. After 56 days of infection, the deep-degree carbonized thick-strip glubam presents better anti-mold properties than medium and non-carbonized specimens. For thin-strip glubam, both parallel and perpendicular to the main bamboo fiber direction were considered. The longitudinal thin-strip glubam retains decent compressive properties, while the transverse specimens stay a stable compressive strength along all fungal tests. The paper reports the experimental values of mass loss, color changes, compressive strengths, modulus of elasticity in compression, and microstructure observations from optical and SEM microscopy at different fungal exposure timespans.

npj Materials Degradation (2023)7:92 ; https://doi.org/10.1038/s41529-023-00407-9

INTRODUCTION

In today's push towards a carbon neutral society, bamboo is gaining wide interest as a potential green material for structural applications, due to its properties of fast growth, lightweight, and low-carbon footprint[1–3]. As an important type of non-wood forest product, many significant industrial applications, in reconstituted forms like laminated panels, have been invented beyond traditional uses of the original round culms. The author's group defined and developed an engineered bamboo for structural purposes called glued laminated bamboo or glubam, or a bamboo-based glued laminated timber[4–6]. The latent capability in the construction area is verified[4,6–9].

In nature, moso bamboo (*Phyllostachys pubescens*) suffers from biologically induced deterioration by fungi such as *Aspergillus niger (A. niger)*, *Penicillium citrinum (P. citrinum)*, and *Trichoderma viride (T. virde)*[10–12]. The mold resistance of glubam is determined by the main ingredient, moso bamboo, which might be more sensitive to fungi than wood-based materials[12–14], given that bamboo is composed of more sugar, starch, protein, and other substances. To determine the degree of fungal induced degradation, mass loss is a typical indicator and results from the degradation of cellulose, hemicellulose, and lignin in bamboo[15]. Xu et al.[16] investigated the chemical structure and microstructure of bamboo, degraded by white-rot and brown-rot fungal for 12 weeks. Several observation methods were used including fourier transform infrared spectroscopy (FTIR) and X-ray photoelectron spectroscopy (XPS), which explained the fungal biodeterioration on moso bamboo specifically. Meng et al.[17] fabricated a composite based on phenol-formaldehyde resin and bamboo fiber for engineered bamboo-related materials. The biological resistance of the bamboo-based fiber reinforced composites was carried out under both white-rot and brown-rot fungi impacts. Several morphological observation methods were employed to analyze the degradation of specimens including fluorescence microscope, SEM with energy-dispersive X-ray, and TEM. Kumar et al.[18] analyzed the resistance of bamboo scrimber against white-rot and brown-rot fungi. White-rot fungi led to a higher average weight loss of specimens than brown-rot fungi. Optical micrographs were demonstrated to show the penetration details of fungal hyphae from the surface into the bamboo scrimber.

Considering the similarity of engineered bamboo- or wood-based materials, the fungal impacts on such materials remain an uncertain issue. Various fungal show different tendencies, resulting in improvement or reduction of the mechanical performances. Liu et al.[19] found that the toughness of bamboo based high-density polyethylene composites increased with the incubation times of the white-rot fungus, *Trametes versicolor*. The typical fungus can reduce the rigidity of raw materials, but enhance the pore volumes, leading to a better interlock between bamboo and plastic. Feng et al.[20] figured out that the fugal degradation caused a lower modulus of rupture, tensile strength, and impact strength, but a higher modulus of elasticity on the wood plastic composites. Crawford et al.[21] found that humidity led to omnipresent fungi on hemp and flax fiber composites, and a longer exposure time destroyed significant mechanical and physical properties of specimens. Clemons et al.[22] confirmed the decrease in flexural strength of wood-filled polyethylene composites after the fungal attack. However, the main reason for the reduction was still

[1]College of Civil Engineering and Architecture, Zhejiang University, Haining, Zhejiang 310058, China. [2]Zhejiang University-University of Illinois Joint Institute (ZJUI), Zhejiang University, Haining, Zhejiang 314400, China. [3]Zhejiang University School of Medicine, Zhejiang University, Hangzhou 310058, China. [4]Zhejiang University - University of Edinburgh Institute, Zhejiang University, Haining 314400, China. [5]Department of Orthopedics of the Second Affiliated Hospital, Zhejiang University School of Medicine, Zhejiang University, Hangzhou 310058, China. [6]Dr. Li Dak Sum & Yip Yio Chin Center for Stem Cells and Regenerative Medicine, Zhejiang University School of Medicine, Hangzhou 310058, China. [7]Beijing Advanced Innovation Center for Materials Genome Engineering, Institute for Advanced Materials and Technology, University of Science and Technology Beijing, Beijing 100083, China. [8]National Materials Corrosion and Protection Data Center, University of Science and Technology Beijing, Beijing 100083, China. [9]BRI Southeast Asia Network for Corrosion and Protection (MOE), Shunde Graduate School of University of Science and Technology Beijing, Foshan 528399, China. [10]Distinguished Qiushi-Chaired Professor of Civil engineering, Director, ZJU-Ninghai Center for Bio-based Materials and Carbon Neutral Development, ZJU-UIUC Joint Institute (ZJUI), Zhejiang University, Haining, Zhejiang 314400, China. [11]Department of Civil and Environmental Engineering, University of Southern California, Los Angeles, CA 90089, USA. ✉email: yanxiao@intl.zju.edu.cn

undetermined because the process of moisture absorption happened during the corrosion process.

With the concern of biological effects of fungal, several treatment methods protect bio-based materials, such as chemical modification by fungicides[23,24] or TiO_2 films[25], physical modification by exterior wood[26] or polymethyl silsesquioxane/Cu-containing nanoparticles xerogel coating[27], oil treatment[14,28–30], and heat treatment[31–34]. Among them, thermal treatment becomes an eco-friendly and effective way to balance fungal durability and mechanical properties of engineered bamboo-based materials. Yang et al verified the fungal resistance improvement after saturated vapor thermal treatment, at 190 °C for 10 h, on bamboo scrimbe[34]. They assessed the infected area of the original bamboo scrimber and heat-treated bamboo scrimber with four types of mold and observed it once a week for 28 days. The method of carbonization was confirmed to improve the mold-proof behavior of bamboo scrimber without any other treatments. Ogutuga et al.[35] pointed out that during the manufacture of laminated bamboo panels, both thicker laminate and thermal treatment can protect laminated bamboo from brown-rot attack. Shangguan et al.[36] studied the physical and mechanical properties of bamboo scrimber after heat treatment, illustrating that the compressive strength reached a peak when the bamboo was carbonized at 170 °C. They figured out that carbonization could solidify the inside adhesives, leading to the enhancement of the physical, mechanical and chemical properties of the bamboo scrimber. Heat treatment can not only help bio-based materials against fungal attacks but also strengthen their stiffness. However, the heat treatment on bamboo-based materials might be strongly adverse. Li et al.[37] found that the bending strength of bamboo bundle curtains decreased by half at 200 °C. There can be a reasonable temperature to balance the mechanical properties and anti-fungal behavior. Brito et al.[38] found that the optimal carbonized condition of heat-treated glued laminated bamboo, based on the adhesive of resorcinol–formaldehyde (RF), should be 160 °C and lasted for one hour to increase the dimensional stability and better performances of axial compressive and bending strengths, compared to other conditions. Schmidt et al. prepared a type of African highland engineered bamboo scrimber that was manufactured and tested the soft rot fungi resistance and stiffness after 3 h heat treatment at temperatures of 160, 180 and 200 °C heat treatment for three hours[39]. The durability of the bamboo scrimber was maintained as first class after the fungal attack. Compared to the untreated specimens, carbonization performed a higher level of fungal resistance and better mechanical performances based on bending tests. One thing that must be pointed out is that the fungal decay procedure would be postponed by the thermal progress, but never terminated.

The durability assessment and the carbonization effectiveness for fungal resistance of glubam are still limited. This study focuses on the *A. niger* deteriorated effects on glubam, which are mainly manifested in the physical, chemical and mechanical properties of density, mass loss, changes of surface colors, microstructures, Fourier transforms infrared spectrometry (FTIR) analysis, and compressive performances such as compressive strength and modulus. The materials used in this research were non-, medium-, and deep-carbonized thick-strip glubam in two directions, including longitudinal and transverse, thin-strip glubam. All specimens were investigated by optical microscope and scanning electron microscopy (SEM), and the compressive properties were explained by quasi-static compression tests.

RESULTS

Mass loss

After different fungal exposure time, the mass loss and the average value for each glubam specimen are shown in Fig. 1. The error bars in Fig. 1 represent the standard deviations based on six specimens, including both three specimens for fungal attack observations and the other three for compressive tests.

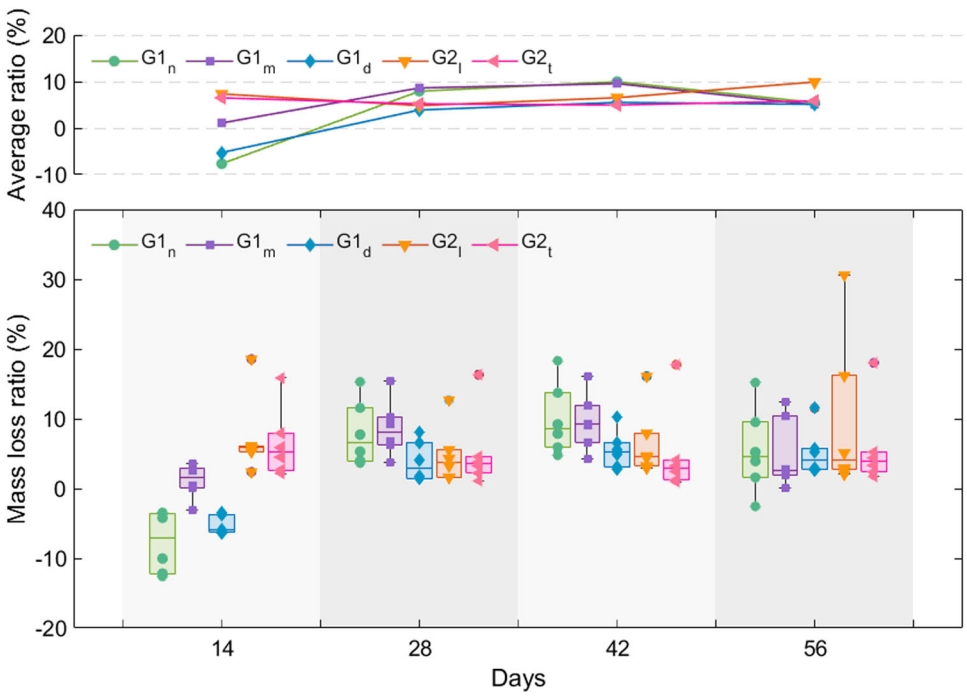

Fig. 1 Time related mass loss of glubam materials. Boxes are colored according to the different median mass loss ratios from five types of glubam. The lower and upper quartiles of mass loss are shown as the bottom and top edges of the box, respectively. The whiskers that extend below and above the box, have endpoints that correspond to the largest and smallest mass losses. Error bars, illustrating the standard deviation, are given for each type of glubam performed. Two-way ANOVA test was used to analyze mass loss in different fungal attack periods and materials. The p-value for this correlation analysis was 0.00 and 0.02, respectively.

The specimens were weighed to calculate the mass loss (ML, %) according to Eq. (1),

$$ML = \frac{M_1 - M_2}{M_1} \times 100 \quad (1)$$

where, M_1 is the matter before incubation (g) and M_2 is the matter after incubation (g). It should be pointed out that specimens from $G1_n$ and $G1_d$ exhibit a slight increase in weight after a 14-day infection. The high temperature and humidity for the cultivation of *A. niger* weight led to an increment in the weights. During the first 14-day infection, the weights of specimens were influenced by the growth of fungus, which consumed the nutrition from both the substrate and specimens. The weight gained from fungus and the loss from the nutrition of bamboo resulted in uncertain changes amongst specimens. Considering the carbonized effects on glubam, compared with the mass loss of $G1_n$, the fungal resistance of $G1_m$ was limited, whilst specimens of $G1_d$ demonstrated effective protection from the fungal attack. From the 14 to 28 days of fungal cultivation, $G1_n$ and $G1_m$ groups lost weight significantly and then decreased slowly after 28 days. As the exposed time goes by, the average mass loss of G2 specimens remained similar from 14 to 56 days, but the standard deviations showed higher fluctuation than G1 materials. A slight decrease in mass loss of G1 materials happened after 56-day incubation, indicating that *A. niger* become in the declining phase. Compared to G2 materials, the cross structure helped more effective fungal growth than the unidirectional arrangement of G1 specimens. Although there is no extra mold-proof method taken place in G2 specimens, the bamboo mats were covered by adhesive to maintain the stability of thin-strip glubam. At the end of fungal decay, the average mass loss of four types of glubam, except $G2_l$, became roughly the same, which showed a 5.36% weight loss. As for the bamboo-based materials, the carbonization or arrangement of bamboo strips had a minor influence on the mass loss when fungi (*A. niger*) exposure continued long enough. The activity of *A. niger* showed a more crucial influence on mass loss, which depends on complex characteristics, such as exhausted nutrients, medium types, and cultural history.

The simultaneous analysis of the interference of the two variables including infection periods and material types on the mass loss was considered through two-wang ANOVA in Table 1. The *p-value* from periods, materials, or interaction is less than 0.05, indicating the significance separately. The results show both variables influent the mass loss significantly. The mass loss performance was impacted by both variables together, due to the interaction *p-value*.

Table 1. Two-way ANOVA test results for mass loss.

Source	Sum of squares	Df	Mean Square	F	*p-values*
Periods	877.44	3	292.48	10.81	0.00
Materials	348.83	4	87.21	3.22	0.02
Interaction	1080.51	12	90.04	3.33	0.00
Residuals	2706.31	100	27.06		

Color changes

Fungal deterioration can cause permanent discoloration on the glubam surface and interior, as shown in Fig. 2. Significant color changes were observed on specimens infected by *A. niger* after 14, 28, 42, and 56 days. With the prolonged exposure time of the fungus, increasing areas of fungal infection were seen by color changes. Remarkably, the discolored places appeared near the bamboo nodes more likely among G1 specimens when the infected surface layer of bamboo contained bamboo strips with nodes. A larger and darker color change area was found on the surface of $G1_n$, compared with $G1_m$ and $G1_d$. The discoloration on the surface of $G1_d$ specimens was lighter, whereas the splits by

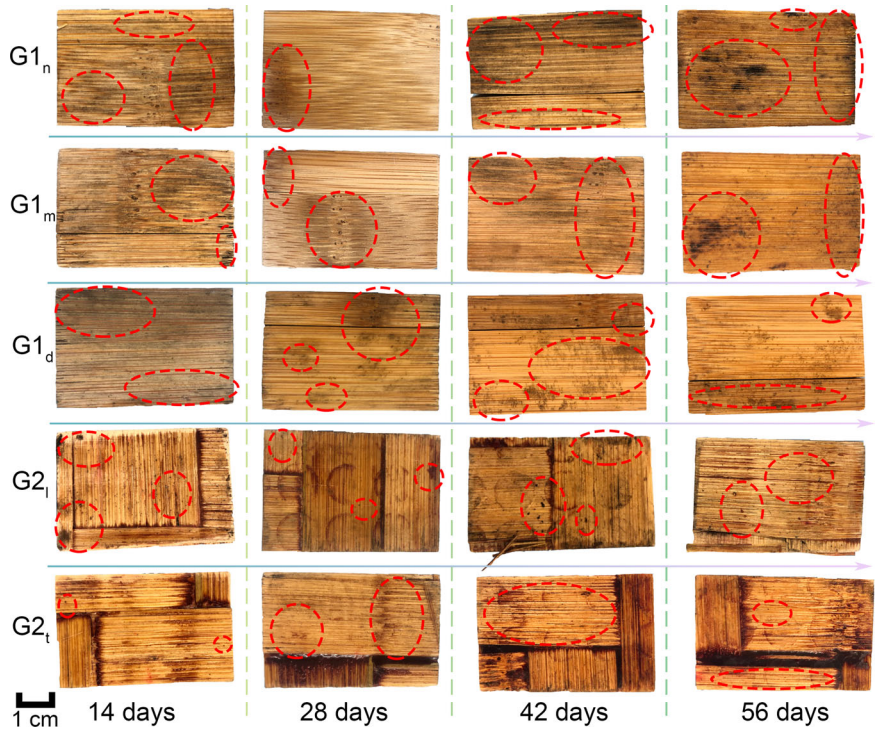

Fig. 2 Typical surface discoloration related to various timespans of glubam. Images showing the color changes in black spots pointed by dotted circles on surfaces from non-carbonized thick-strip glubam ($G1_n$), medium-carbonized thick-strip glubam ($G1_m$), deep-carbonized thick-strip glubam ($G1_d$), longitudinal thin-strip glubam ($G2_l$), and transverse thin-strip glubam ($G2_t$) after 14-, 28-, 42-, and 56-day fungal attack.

Table 2. Mean and standard deviation of compressive strength (MPa) and modulus of compression (GPa).

Days	(MPa)	$G1_n$		$G1_m$		$G1_d$		$G2_l$		$G2_t$	
	(GPa)	Mean	SD	Mean	SD	Mean	SD	Mean	SD	Mean	SD
0	Strength	59.84	4.80	83.35	1.57	88.05	3.48	68.60	12.27	24.03	2.45
	Modulus	8.83	0.31	12.06	4.60	12.79	1.77	10.49	1.51	8.32	4.11
14	Strength	36.78	2.37	48.27	6.54	48.40	0.88	51.13	1.96	19.18	3.68
	Modulus	6.63	1.37	8.10	1.38	8.46	0.91	11.31	5.78	6.84	1.99
28	Strength	39.07	1.05	47.52	3.59	59.45	3.74	43.06	2.59	17.51	6.26
	Modulus	7.42	0.45	8.10	1.14	10.00	1.05	8.77	3.10	4.83	0.50
42	Strength	37.92	2.72	44.61	2.89	63.18	2.10	46.49	1.85	16.51	4.03
	Modulus	6.02	0.74	8.31	0.27	14.16	3.60	12.65	4.37	7.23	2.53
56	Strength	26.98	0.72	38.85	1.19	64.35	2.63	48.01	1.39	17.32	0.61
	Modulus	5.94	0.61	8.68	1.15	8.69	1.53	10.14	4.19	8.35	3.10

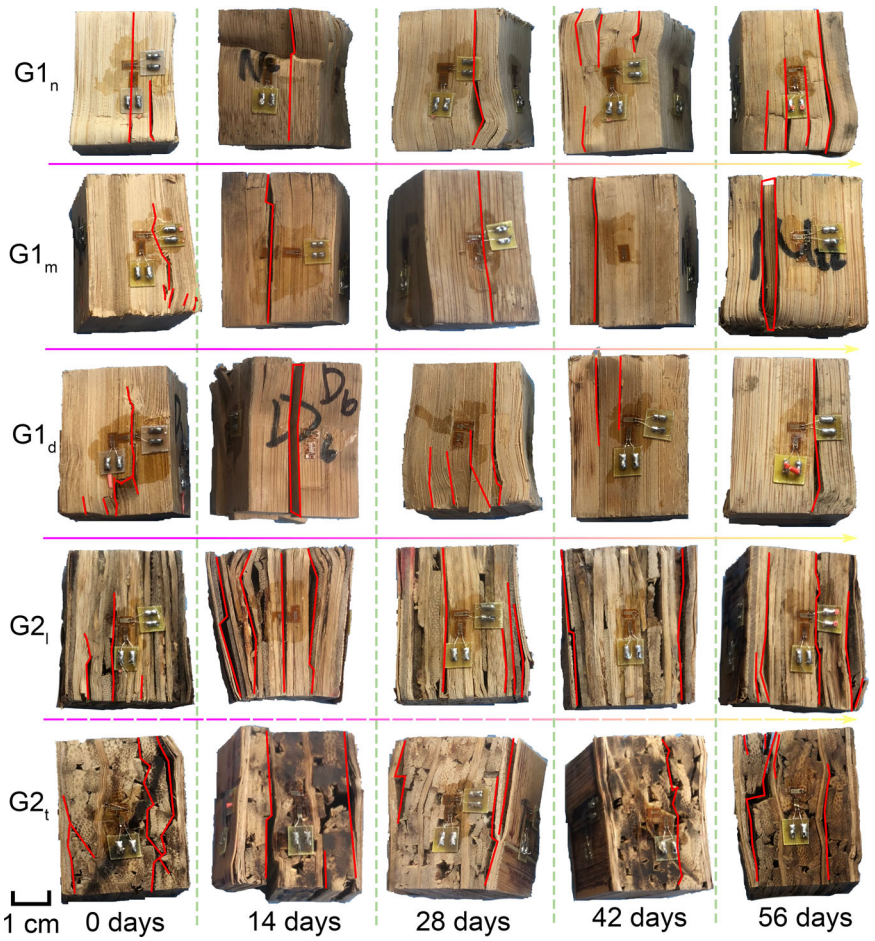

Fig. 3 Typical failure modes after compressive tests. Images showing the failure modes from non-carbonized thick-strip glubam ($G1_n$), medium-carbonized thick-strip glubam ($G1_m$), deep-carbonized thick-strip glubam ($G1_d$), longitudinal thin-strip glubam ($G2_l$), and transverse thin-strip glubam ($G2_t$) after 0-, 14-, 28-, 42-, and 56-day fungal attack. Red lines are the outlines of cracks.

degumming occurred more frequently. Compared with G1 specimens, the surface color of G2 specimens was less obvious and discrete.

Compressive behavior

The experimental results from compressive tests after fungal attacks are shown in Table 2 for the compressive strength and modulus of elasticity. Comparisons among different glubam materials and different fungal attack time can be conducted.

Figure 3 illustrates the typical failure modes of thick- and thin-stirp glubam materials. The delamination was noticed for all types during the tests, which leads to splitting of the bamboo strip layers. Due to the one-direction attack, the fungal contact surface of glubam specimens exacerbated the property of asymmetry, which leads to eccentric compression. The type of wedge splits was also noted in both top and bottom of specimens. The out-of-

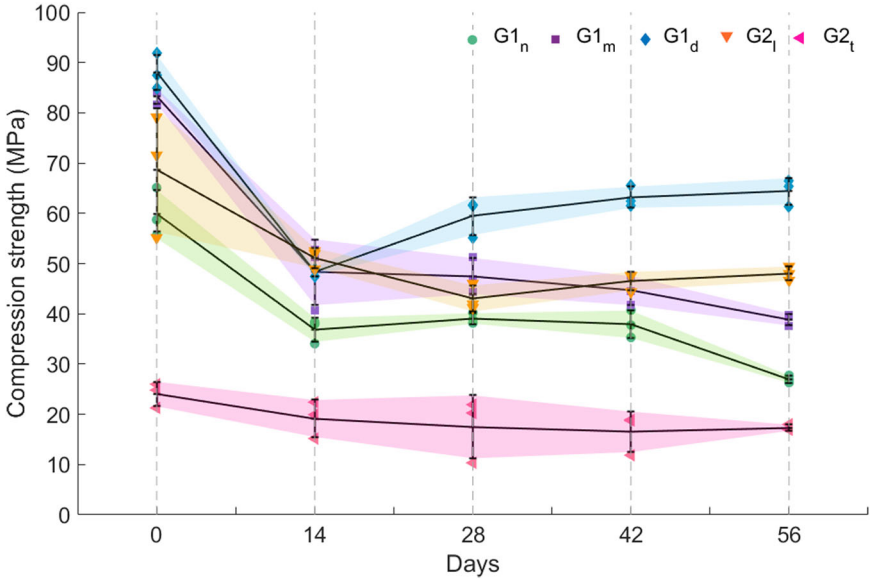

Fig. 4 Compression strength of glubam related to time. Error bars, illustrating the standard deviation, are given for each type of glubam performed.

plane fiber buckling failure occurred in G1 specimens, whereas the in-plane fiber buckling failure was carried out in $G2_l$ materials. For $G2_t$ specimens, the cracks extended porous defects without adhesive. The temporal influences on G1 and G2 specimens were limited from 14 to 56 days of infection but compared with the control group without fungal tests, more cracks after failure would be found. In addition, the carbonized pretreatment appears to have a slight influence on the failure modes, which led to more significant splits. The overarching failure modes were quite similar, characterized by splitting and localized crushing near the compressed ends of the specimens. Most cracks developed along the vertical length direction of the specimen with the loading.

The following Eq. (2)[40] and Eq. (3)[41] are applied to assess the compressive behaviors,

$$\sigma_w = \frac{P_{max}}{bt} \tag{2}$$

$$E_w = \frac{\Delta P}{b \times t \times \Delta \varepsilon} \tag{3}$$

where, σ_w is parallel to grain compressive strength in MPa; P_{max} is the maximum load value in N; b is the width of the specimen in mm; t is the thickness of specimen in mm; E_w is the modulus of elasticity; ΔP is the range of the loadings from the upper and lower limits, and $\Delta\varepsilon$ is the increment of the corresponding strains.

The compressive strengths can be assessed by Eq. (2), and shown in Fig. 4. Compared with the results of the control group, the mold impacted on thick- and thin-strip glubam obviously. G1 and $G2_l$ specimens have a strength degradation after the first 14-day fungal tests, reaching 38.54% ($G1_n$), 42.09% ($G1_m$), 45.03% ($G1_d$), and 25.47% ($G2_l$), respectively, whilst, $G2_t$ only degraded by 20.20%. Notably, the compression strengths of $G1_m$, $G1_d$, and $G2_t$ specimens showed a slight increase as time went by. It is reasonable that the stability of $G2_t$ strengths is beneficial from the transverse alignment. More possible voids without adhesives in $G2_t$ led to a more uniform fungal distribution. Considering the growth of *A. niger*, the specimens experienced larger numbers of fungi after a longer time, indicating that less nutrition from glubam can feed them. After the turning point of compressive strengths, such as 14-day infection for $G1_d$ and 28-day infection for $G2_l$, some *A. niger* lost activities, and deep-carbonization strengthen thick-strip glubam by diminution of the content of hemicellulose, pentose, and other chemical materials, which would restrict the fungal development. It is suspected that the growth of *A. niger* filled in the porous bamboo fabric structures resulted in the increased compression strength of $G2_l$ from 28 days to 56 days of infection. The heat treatment played a crucial role in the mold-proof characteristic from the view of compression strength results, in which the $G1_d$ remained as much as possible compressive resistance after 56-day fungal deterioration.

Figure 5 shows the modulus of elasticity in compression and averages evaluated in glubam, based on the calculation of Eq. (3). Besides $G1_n$, the final remained modulus of elasticity presented similar, which were 8.68 GPa ($G1_m$), 8.69 GPa ($G1_d$), 10.14 GPa ($G2_l$), and 8.35 GPa ($G2_t$), respectively. The fungal attack modulus of elasticity in compression on $G1_n$ specimens was demonstrated destructively. The modulus of elasticity in compression of medium carbonized thick-strip glubam remained stable during the against of *A. niger*, indicating that the timespan effect on $G1_m$ was limited. The compression property of $G1_d$ after 14-day exposure presented an irregular behavior, which increased at 28 and 42 days then and decreased rapidly. Compared to the untreated specimens, medium and deep carbonized pretreatments protected glubam from fungal deterioration.

As for thin-strip glubam, the average modulus of elasticity in compression performance of $G2_l$ showed uncertain tendencies from the infection start, caused by the huge variations amongst three replicates in each group. The quality control of longitudinal thin-strip glubam should be considered more in further works. Taking the medians of $G2_l$ specimens into account, the peak arrived at a group of 42-day attacks, which means $G2_l$ specimens would survive more values of compression modulus to resist a longer time of fungal deterioration. The modulus of elasticity in compression of $G2_t$ increased after 28 days, similar to the performances of compression strengths but showing more significance by the modulus.

From the statistical analysis, shown in Table 3, the results show both periods and material types interfered in compression modulus significantly. The interaction ($p > 0.05$) means that the mutual influence of two independent variables, fungal attack periods and different glubam materials, on the compression modulus is insignificant.

With the application of a total of eight stain gauges glued on the side faces of each specimen, Poisson's ratio can be calculated from Eq. (4). It is notable that the existing uncertainty to assess the

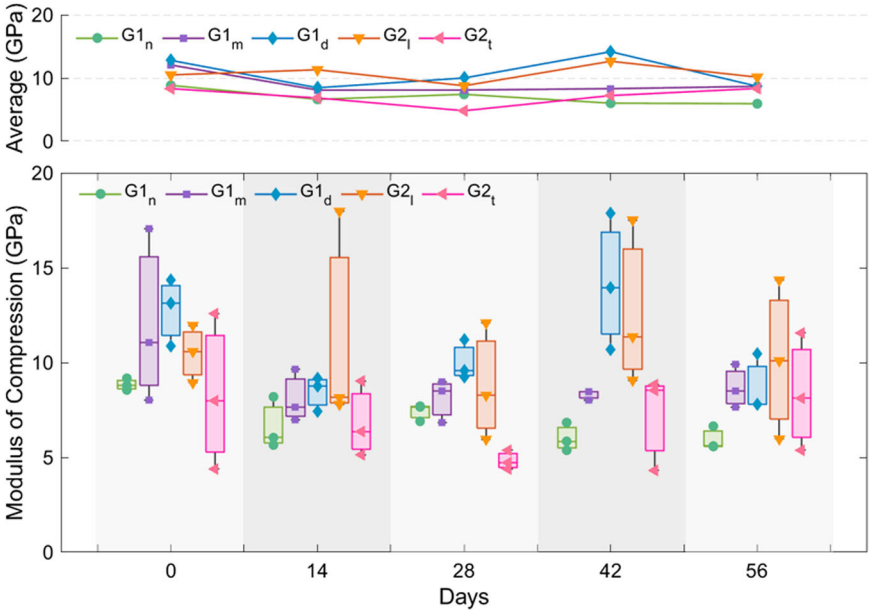

Fig. 5 Modulus of compression of glubam related to timespans. Boxes are coloured according to the different median modulus of compression from five types of glubam. The lower and upper quartiles of modulus of compression are shown as the bottom and top edges of the box, respectively. The whiskers that extend below and above the box, have endpoints that correspond to the largest and smallest modulus of compression. Error bars, illustrating the standard deviation, are given for each type of glubam performed. Two-way ANOVA test was used to analyze compression modulus in different fungal attack periods and materials. The p-value for this correlation analysis was 0.04 and 0.00, respectively.

Table 3. Two-way ANOVA test results for compression modulus.

Source	Sum of squares	Df	Mean Square	F	*p-values*
Periods	74978284.01	4	18744571.00	2.79	0.04
Materials	206492535.36	4	51623133.84	7.67	0.00
Interaction	103937461.57	16	6496091.35	0.97	0.51
Residuals	336420870.58	50	6728417.41		

Table 4. Average Poisson's ratio of glubam.

Days	0	14	28	42	56
$G1_n$	0.33	0.12	0.31	0.26	0.23
$G1_m$	0.32	0.33	0.24	0.37	0.34
$G1_d$	0.26	0.53	0.35	0.38	0.13
$G2_l$	0.52	0.15	0.35	0.33	0.30
$G2_t$	0.22	0.35	0.37	0.27	0.20

Poisson's ratio of anisotropic materials, glubam. According to Eq. (4), a simplified experimental test was carried out.

$$v = -\frac{\varepsilon_{trans}}{\varepsilon_{axial}} \tag{4}$$

Where v is the Poisson's ratio, ε_{trans} is the transverse strain, and ε_{axial} is the axial strain.

Due to the fungal attack pattern, one side was exposed, which indicates that the after-corrosion specimens suffered from eccentric compression. To simplify the calculation, the data from two orthometric strain gauges on each side averaged, listed in Table 4. Fungal degradation had a minor impact on Poisson's ratios of five groups. However, a higher degree of carbonization led to a large value of Poisson's ratio.

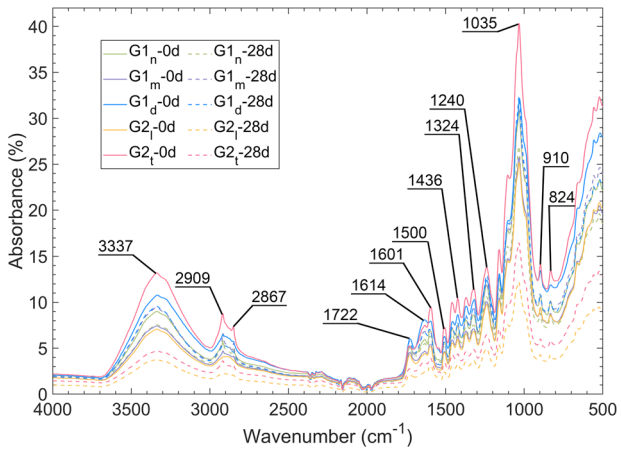

Fig. 6 FTIR spectrum of glubam slices without fungal deterioration and with 28 days fungal deterioration. The solid lines represent the FTIR spectrum of five types of controlled glubam. The dotted lines represent the FTIR spectrum of five types of 28-day fungal attacked glubam.

FTIR analysis

Figure 6 illustrates the characteristic absorption bands of various chemical groups. Five types of glubam small specimens were analyzed, including those without fungal attack and those subjected to a 28-day fungal attack. The impact of fungal deterioration varied among different glubam specimens. While the peaks of thick-strip glubam (G1) specimens showed limited changes, significant variations were observed in the thin-strip glubam (G2) specimens. At the wavenumber 3337 cm^-1, broad bands were evident, signifying the presence of hydrogen (OH-) bonded stretching associated with cellulos I_β in bamboo. This same wavenumber indicated the NH stretching mode, suggesting the presence of polysaccharides, amine, amide groups in *A. niger*,

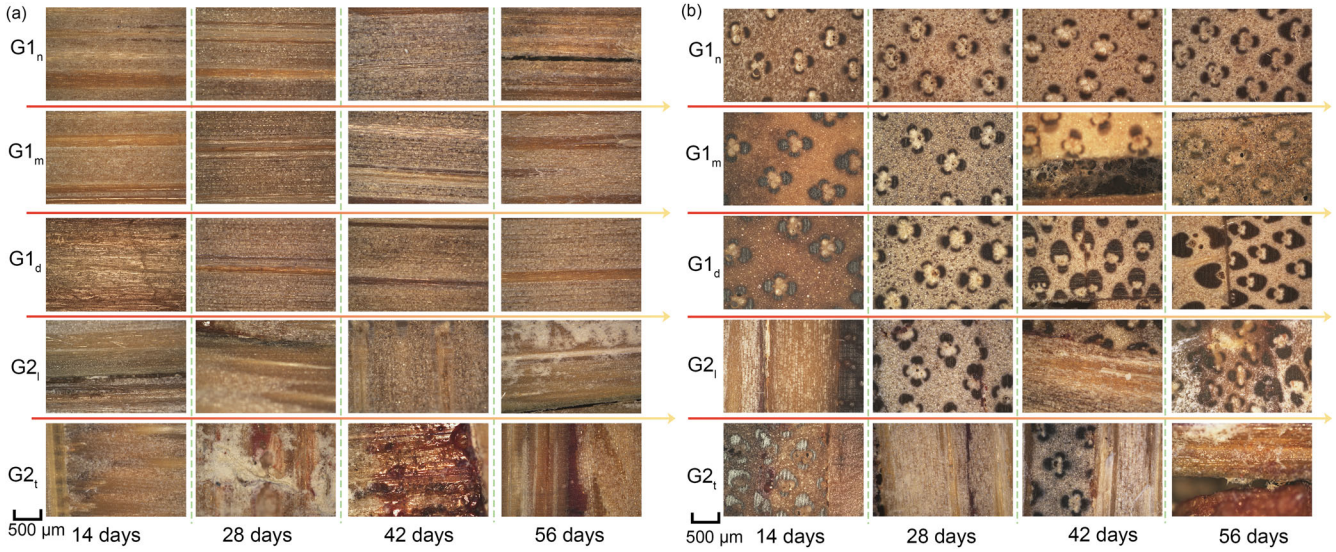

Fig. 7 Optical micrographs of the corrosion morphology from typical glubam (5×). a Longitudinal glubam slice surfaces from 10 mm below infected surfaces. **b** Transverse glubam slice surfaces from 20 mm to the left side.

as well as NH stretching vibrations in phenol adhesives or urea resin. The bands at 2909 cm^-1 and 2867 cm^-1 correspond to *ν*(C–H) vibration, indicative of the presence of cellulose and hemicellulose in bamboo. The absorption band at 1722 cm^-1 characterizes stretching vibration C=O and -COOH groups in hemicellulose, as well as aliphatic aldehydes (formaldehyde) from urea resin. The absorption bands at 1614 cm^-1, related to C=O stretching, confirmed the presence of absorbed water and amide in adhesives. At 1601 cm^-1, aromatic ring in lignin can be confirmed with the C=C group. Compared to the bands at 1500 cm^-1, guaiacyl elements were more pronounced than syringyl in lignin. The peak at 1436 cm^-1 indicated aromatic skeletal vibrations (C-H, CH2) in lignin and symmetric bending in cellulose. This peak also confirmed the existence of COO- groups associated with the fungal. The O-H bending in cellulose of bamboo can be found at 1324 cm^-1. As to resins, C-H band confirmed the presence of methyl. Guaiacyl ring breathing with CO-stretching in lignin and hemicellulose of bamboo or *A. niger* took place in peaks at 1240 cm^-1. Aromatic C-H in-plane deformation of cellulose in bamboo can be found at 1035 cm^-1. C-O stretch in methylol appeared at the same location in UF. The vibrational type at 910 cm^-1 was attributed to the pyranoid ring (C-H) in cellulose and hemicellulose, while C-H deformation in cellulose was observed at 824 cm^-1 in bamboo.

The components of cellulose and hemicellulose were related to the main part of supporting force. There is a slight increasing of FTIR spectrum from $G1_n$-0d and $G1_m$-0d to $G1_n$-28d and $G1_m$-28d, due to the active fungal. The situation can be explained the similar performance of mass loss ratio and modulus of compression in $G1_n$-28d and $G1_m$-28d. It is notable that the deep-carbonized glubam ($G1_d$) performed an insignificant error between specimens after deterioration and original condition. FTIR spectrum can verify the limited changes of compressive properties in $G1_d$ materials. The differences between 28 days and non-fungal attacked G2 specimens were crucial, indicating the substantial fluctuations in modulus of compression.

Optical microscopy

The optical micrographs of five groups are exhibited in Fig. 7, in which the specimens from each group with various infection timespans were sliced by a diamond wire cutting machine along both laminated direction (x-z plane) and transverse direction (x-y plane) in Fig. 7a, b, respectively. Considering the dimensions of slices, a 5× lens was used to look into typical surfaces. The color differences from various carbonized degrees and various time-spans of G1 specimens are difficult to be distinguished. However, increasing black stains by fungal infection is significant with a longer time of G1 groups in Fig. 7a, whilst, it is dramatically observed from the first 14 days to the end of infection of $G1_n$ in Fig. 7b. Compared with G1n and $G1_m$, transverse optical micrographs, the fungal affected areas are limited after 56 days of exposure.

As for G2 specimens, the porous manufacturing structure led to huge space for *A. niger* to live. For example, in Fig. 7b, $G2_l$-56d captured the prospect white or yellow hypha, which would turn to black[42].

With the characteristic of *A. niger*, the type of mold was confirmed that it would produce both cellulase and *β*-xylanase[43], which indicates that the fungus consumed the nutrition and left holes in specimens, like $G1_m$-42d. It is worth noticing that the capacity of offering the cellulase enzyme by *A. niger* decreased the mechanical properties of bio-based materials more.

The details of *A. niger* impacts on bamboo are shown in Fig. 8, in which both longitudinal and cross-section optical micrographs are considered. It is noticeable that the optical micro photos of cross-sections are more visible than those of radial sections. For bamboo fibers, Fig. 8a, b illustrate that *A. niger* can degrade cellulose, where black spots existed in the fiber bundles. The inside of $G1_{m-1}$-56d was covered with fungus not only on the matrix but also on the pictured void in Fig. 8d.

SEM microscopy

After 28 and 56 days of exposure, the SEM images of five groups of glubam specimens were taken and shown in Fig. 9. The fungus of *A. niger* colonized on the glubam surface and inside parenchyma cells (matrix) and conductive tissues (voids)[44], shown in Fig. 9a to c. The surface of specimens was cleaned by alcohol cleansing wipes but the hypha was distributed everywhere and grew up from holes of $G2_l$-28d. Compared with $G1_n$ and $G1_m$ specimens, the fungus developed mildly in $G1_d$, $G2_l$ and $G2_t$ indicating that the deep carbonization and the orthometric fiber manufacture restrained the growth of *A. niger*.

On the other hand, the colonization of *A. niger* is unnoticed by the end of the experiment compared with the micrographs of 28-day infected specimens, demonstrated in Fig. 9f to j. After 56 days the decay was slow due to the lack of nutrition to cultivate fungus.

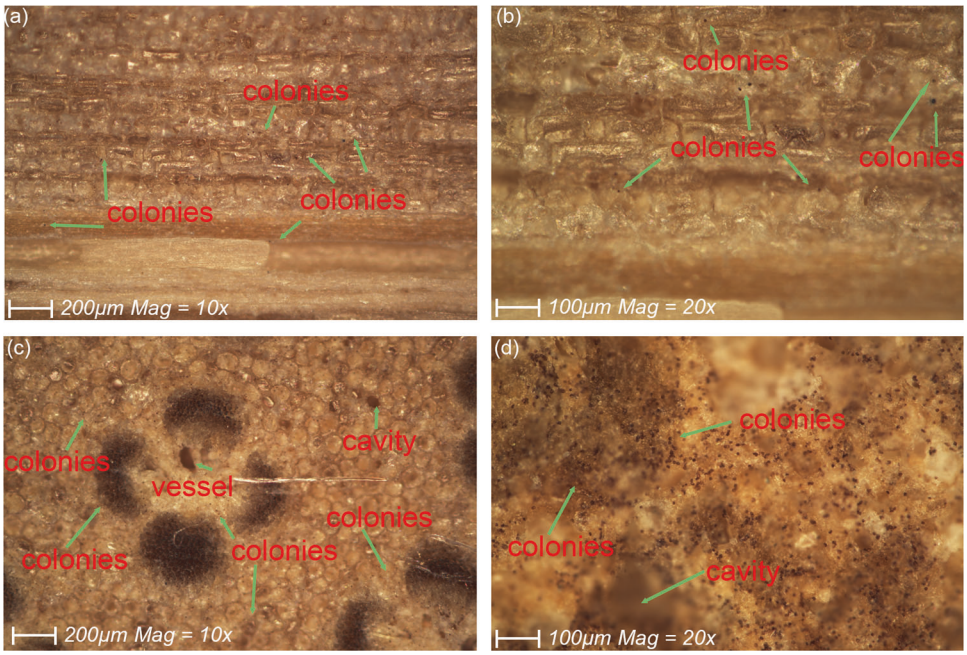

Fig. 8 Typical optical micrographs of medium-carbonized thick-strip glubam after 56-day fungal attack ($G1_m$-56d). **a** Longitudinal section of $G1_{m\text{-}6}$-56d with 10 magnifications. **b** Longitudinal section of $G1_{m\text{-}6}$-56d with 20 magnifications. **c** Cross-section of $G1_{m\text{-}1}$-56d with 10 magnifications. **d** Cross-section of $G1_{m\text{-}1}$-56d with 20 magnifications.

The micro views pointed out another important information that *A. niger* was capable of producing cellulase. The appearance of bamboo fibers became rough and uneven, and the boundaries of parenchyma cells were blurry. Those are the evidence of damage to the bamboo structures. More transparent cracks and gaps were emerging in Fig. 9g, h, and j, indicating the failure happened in the longitudinal in the first period and then transversely.

The longitudinal-section SEM micrographs of five groups of glubam at the end of fungal tests are shown in Fig. 10. After a 56-day fungal attack, the results indicate that both cavity formation and erosion decay took place, where the cell walls thinned and discrete notches appeared, as shown in Fig. 10a. The colonization of fungal hyphae resulted in disorder and unsystematic fiber bundles, due to the consumption of matrix first in Fig. 10b. Most cell walls are affected and fragmented. From the longitudinal view of the $G1_d$ specimen, the inner structure of the parenchyma cell in the green circle was noticed. Based on the bidirectional fiber manufacture, the surface of the selected $G2_l$ specimen remained smooth and wrapped in the matrix, compared with other groups in Fig. 10d. After 56 days advanced stage of decay was observed, and the cell wall was eroded, due to the extensive degradation in Fig. 10e.

DISCUSSION

Aspergillus niger can cause permanent discoloration on the glubam surface, which leads to the fungus called black mold. According to the color changes, a computational approach was used to qualify the area of infection, based on MATLAB. (R2022b). The processing procedure is illustrated in Fig. 11, by taking the specimens of the $G1_m$ group for example. The original photo of the exposure surface was taken under similar surroundings and uniform light irradiation. All the original photos were converted into gray images, which extracted the most important information about black areas. Based on the gray photo, the grayscale contour can be inducted numerically.

For example, a total of six specimens is demonstrated in Fig. 11, each grayscale contour was aligned and departed into three segments. Small values of the grayscale represent possible bamboo nodes or defects as the dark zone. The large values from the bright zone of grayscales were recognized as the bamboo surface remained the original color. Besides, the surface degradation was figured out in the selected zone. The thresholds between the two sectors would be reconstructed for each group.

In terms of computational programs, the surface degradation can be assessed in Table 5. As the fungal attack continued, $G1_n$ performed a constant increase in the color change areas. The peak ratio of infection to whole surface areas assessed by computer appeared after different fungal colonized timespans. During the first 14 days of tests, $G2_l$ performed better fungal resistance than other groups, in which the other four groups showed roughly the same area of infection. The limited infected areas of $G1_m$ and $G1_d$ groups can explain the tendency of compressive properties from the discolored point of view, which indicates that the mechanical estimate of antifungal glubam specimens can be verified by picture processing. Carbonization appears to be an effective pretreatment method to protect glubam from *A. niger* impacts. The large ratio of color changes on transverse thin-strip glubam occurred in every fugal experimental stage, due to the poriferous alignment structure offering abundant living spaces for *A. niger*.

Regression analyses of the relations between surface degradation portions from the image estimation by computer and ultimate strengths by compressive tests can be shown in Fig. 12. The 95% confidence interval of each group is demonstrated by the shadow area. It is noticeable that the compressive strengths of specimens decreased obviously, mainly due to the large area of fungal infection. The decreasing tendency illustrates the possibility of connecting the degradation areas to strengths directly. However, it is troublesome to quantify the strengths by linear equations accurately, with the consideration of the unsatisfied coefficient of determination and 95% confidence interval, shown in Fig. 12. The reliability of the fitting curve is limited by the consideration of irregular surfaces, especially for G2 specimens. In further works, promising fitting equations could be modified by more testing specimens and a better imagination procedure.

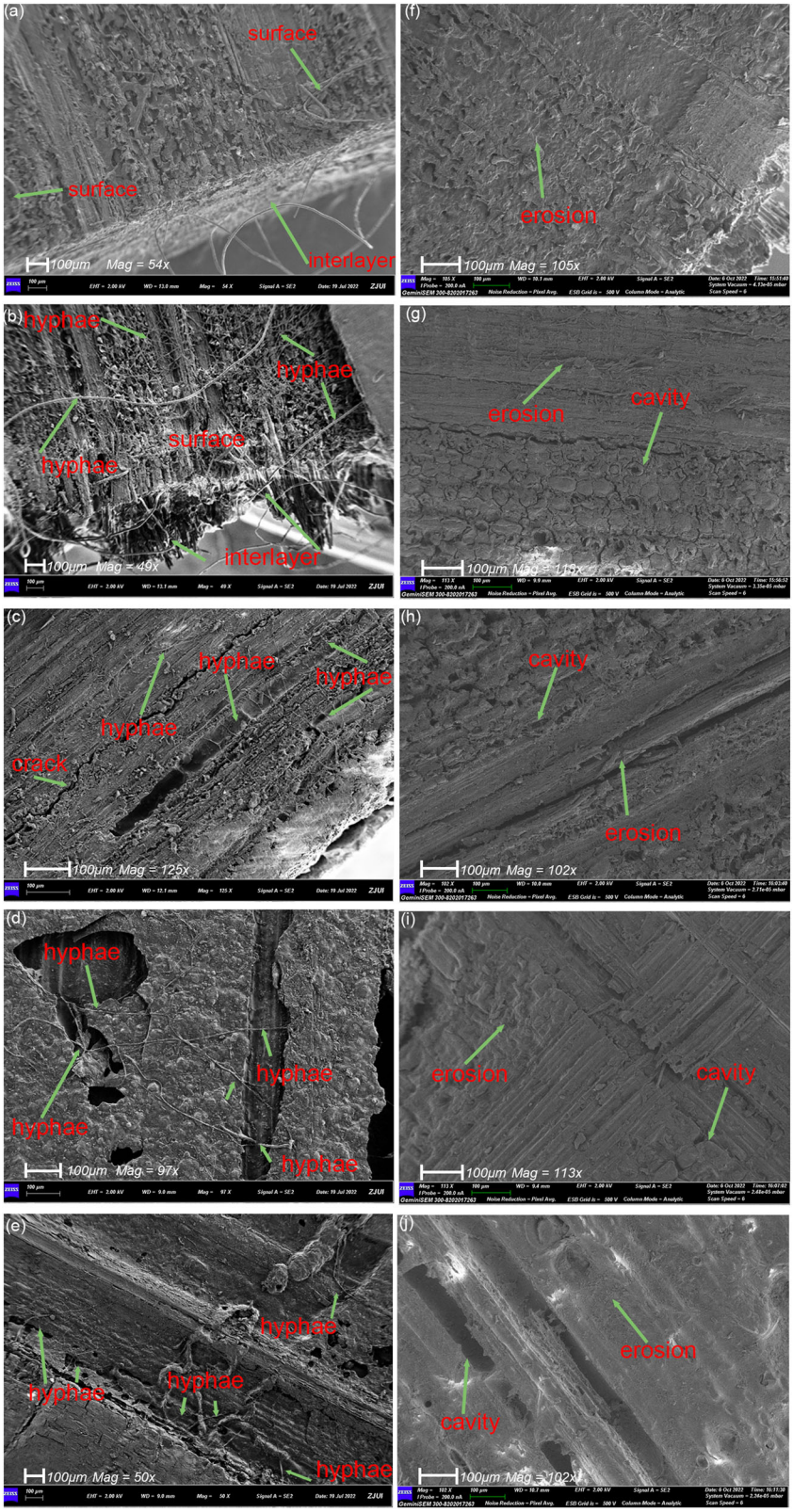

Fig. 9 SEM photos of glubam specimens inoculated with *A. niger*. **a** $G1_n$-28d. **b** $G1_m$-28d. **c** $G1_d$-28d. **d** $G2_l$-28d. **e** $G2_t$-28d. **f** $G1_n$-56d. **g** $G1_m$-56d. **h** $G1_d$-56d **i** $G2_1$-56d **j** $G2_t$-56d. The hyphae on the surface and interlayer, fungal attacked erosion and cavity are pointed.

In this study, the effect of fungal (*Aspergillus niger*) degradation on the compressive performances of glubam was studied, in which the heat-treated thick-strip and orthometric thin-strip glubam were considered. A series of physical, mechanical and microcosmic observations were carried out for five types of glubam, including non-carbonized thick-strip glubam ($G1_n$), medium-carbonized thick-strip glubam ($G1_m$), deep-carbonized thick-strip glubam ($G1_d$), longitudinal thin-strip glubam ($G2_l$), and

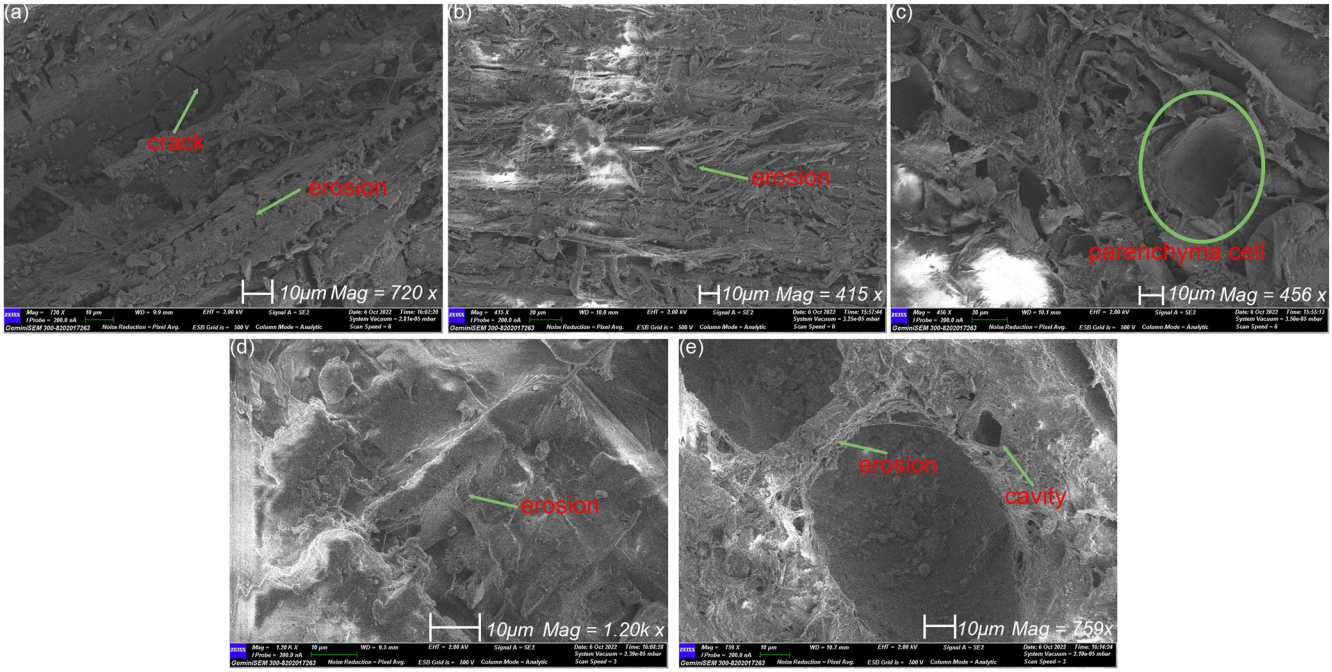

Fig. 10 Typical radial-section SEM micrographs of five groups of glubam after 56 days of fungal attacks. a $G1_{n\text{-}6}$-56d. **b** $G1_{m\text{-}6}$-56d. **c** $G1_{d\text{-}6}$-56d. **d** $G2_{1\text{-}6}$-56d. **e** $G2_{t\text{-}6}$-56d. The fungal-attacked crack and erosion are pointed. The significant parenchyma cell is circled.

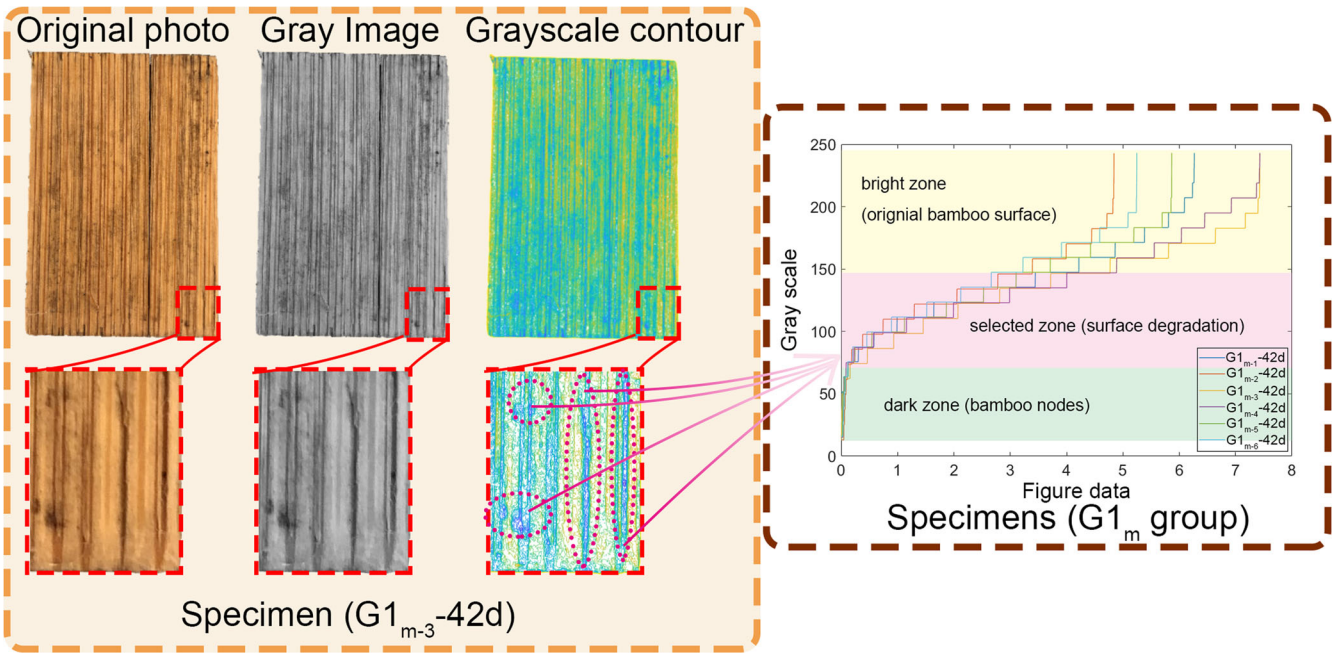

Fig. 11 Surface degradation assessing processes by computer from $G1_{m\text{-}3}$-42d and computational results from $G1_m$ group. The left side demonstrates the image procedure of $G1_{m\text{-}3}$-42d based on the grayscale image. The right side explained the image numeralization with the threshold of surface degradtion of $G1_m$-42d group.

transverse thin-strip glubam ($G2_t$). The main conclusions can be drawn as follows:

(1) The mass loss of each type of glubam material was uncertain. Specimens from thick-strip glubam performed an analogous tendency in mass loss, where the mass lost rapidly from 14 to 28 days of infection and arrived at the peak after 42 days. The mass loss of $G2_l$ became irregular from the beginning to the end. On the contract, the mass loss of $G2_t$ remained stable as time went by.

(2) Aspergillus niger was verified to cause surface color changes in every group of glubam materials. The heat treatment protected thick-strip glubam from dramatic discoloration, compared $G1_m$ and $G1_d$ to $G1_n$ specimens. The surface of thin-strip glubam remained the most original surface color and discrete speckles appeared rather than continuous black

colonies in G1 specimens. A consequent computational method by MATLAB (2022a) was applied to assess the infected areas quantitatively.

(3) The compressive behaviors of glubam are conducted, including failure modes, compressive strength, and modulus of elasticity in compression. The thermal treatment influences the failure modes of thick-strip glubam finitely, whilst the transverse glubam showed more cracks than longitudinal specimens.

(4) As for compressive strength, due to the activity of fungus, the first 14-day fungal attack all specimens extremely. The deep degree of carbonization helped thick-strip glubam survive from serious destruction of compressive strength. A slight increase emerged after 28 days of infection like $G1_d$ and $G2_l$, due to the growth of fungus fulfilled the original drawbacks of glubam materials. Compared to $G2_t$ specimens, $G2_l$ kept a higher level of compressive strength. However, the merit of $G2_t$ material is that the effects of *A. niger* on compressive strength are slight.

(5) The optical micrographs of longitudinal and transverse sections from character glubam slices were conducted. The existence of *A. niger* was more likely to be detected in the transverse graphs than the longitudinal ones from the first 14 days to the end of fungal tests. From megascopic optical observations, fungus generated cellulase enzymes that expanded in bamboo fibers rather than parenchyma cells.

(6) The morphological characteristics of glubam decay by *A. niger* were investigated using SEM. It is remarkable the fungal hyphae grow up in bamboo matrix and fibers, come out of the defects of glubam, and adjoined on vessels. Both cavity formation and erosion decay happened.

Table 5. Surface color degradation area portions.

Name	14d		28d		42d		56d	
(%)	Mean	SD	Mean	SD	Mean	SD	Mean	SD
$G1_n$	15.77	8.49	19.46	6.62	20.68	7.55	33.23	4.38
$G1_m$	15.94	9.13	4.04	1.61	13.58	2.33	22.88	9.33
$G1_d$	15.44	6.92	8.07	4.01	8.73	5.60	7.01	4.06
$G2_l$	7.35	2.36	12.54	3.52	18.32	7.83	13.74	3.44
$G2_t$	15.55	2.65	14.30	2.60	15.45	7.63	20.13	4.47

METHODS

The fungal attack tests were carried out with *A. niger* for glubam specimens. The quasi-static compressive strength and modulus of elasticity of glubam boards with different degrees of fungal attack were examined using a universal loading testing machine.

Preparation of engineered bamboo specimens

The preparation of glubam contained a two-step lamination process[1,7,9]. The first process is to integrate the bamboo strips into the large size and standardized board, through a hot-pressure process, under ~5 MPa pressure and 150 °C temperature, which owns a typical plate size of about 2000 to 2500 mm in length (or longer), and 600 to 1200 mm in width. The second process is pressure lamination of the elements cut from the boards at room temperature. The essential ingredients of glubam were 3 to 6 years old moso bamboo (*Phyllostachys pubescens*), urea formaldehyde adhesive (for thick-strip glubam) and or phenol formaldehyde adhesive (for thin-strip glubam). The second process is to

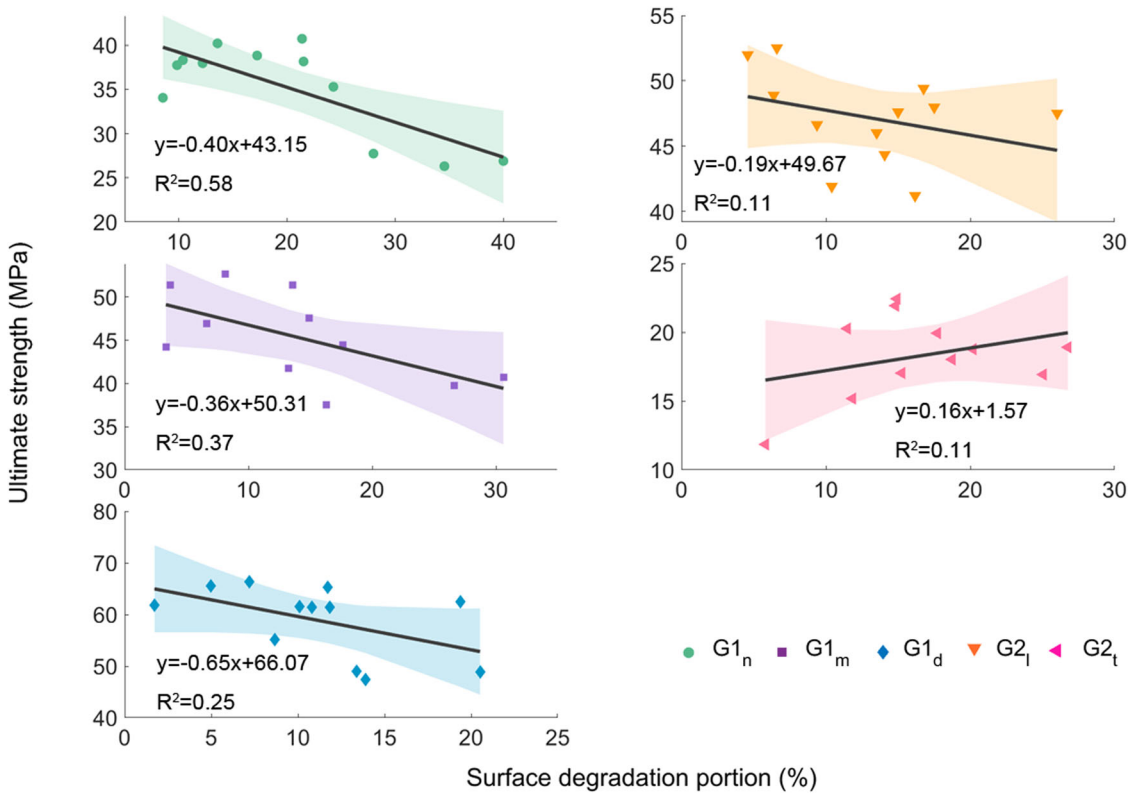

Fig. 12 Regression analysis of the relations between surface degradation portions and ultimate strengths. One-way ANOVA test was used to analyze ultimate strengths in different fungal deterioration areas. The p-value for this correlation analysis was 0.00, 0.00, 0.00, 0.00 and 0.42, respectively correspond $G1_n$, $G1_m$, $G1_d$, $G2_l$ and $G2_t$.

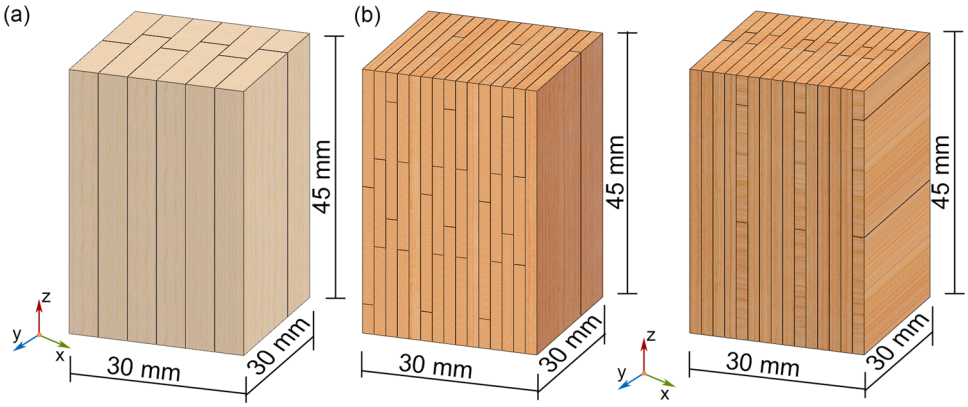

Fig. 13 Specimen schematics of glubam. a Thick-strip glubam, G1. **b** Thin-strip glubam in two directions, G2. The dimension of the specimens is shown.

Table 6. Details of specimens.

	Geometric dimensions (mm)	Characteristic	Average density /SD (oven-dry) (kg/m^3)	Average density / SD (test) (kg/m^3)
G1	30 × 30 × 45	Non	565.7 / 28.5	658.8 / 43.4
		Medium	635.2 / 45.2	728.5 / 63.2
		Deep	742.7 / 17.6	819.7 / 35.5
G2	30 × 30 × 45	Longitudinal	822.9 / 52.2	941.7 / 116.5
		Transverse	810.6 / 52.3	903.2 / 73.0

produce structural components using engineered bamboo boards by a cold-press lamination process with phenol adhesives or urea resin. In this study, the specimens were made by cutting the engineered boards. The thick-strip laminated glubam board is made by pressing several layers of 5 ~ 8 mm thick and 200 mm wide bamboo strips, while the thin-strip laminated glubam sheets are made by laminating ~2 mm thick bamboo strip mats to have a total thickness of about 10 to 35 mm. The thin strips are netted and dried to reduce their water content below 10 ± 2%. All the strips are saturated in adhesives for about 2 to 3 min, and consequent by drying again to control the moisture content in a range of 16 ± 2%. The two types of glubam specimens are illustrated in Fig. 13. The thick-strip glubam shown in Fig. 13a, nominated as G1, had six layers aligned in parallel to bamboo fiber with a total thickness of 30 mm. The thin-strip glubam designated as G2, contains 15 layers of orthometric thin bamboo mats, in which the longitudinal-transverse ratio of bamboo fiber is 4:1, shown in Fig. 13b. All the specimens owned the same geometric dimensions of 30 mm × 30 mm × 45 mm. The direction of parallel-to-grain bamboo fibers was also the long side of G1 specimens.

Two degrees of carbonized and one controlled conditions were used to produce G1 specimens. Based on the different carbonized temperatures, G1 specimens can be categorized as non-carbonized G1 ($G1_n$), medium-carbonized G1 ($G1_m$), and deep-carbonized G1 ($G1_d$). The medium degree of steam heat treatment on G1 materials was at 175 °C for 90 min and the deep one was 185 °C for 90 mins. As for G2 specimens, there was no extra carbonized process conducted but the orthometric cutting directions were considered amongst G2 materials, shown in Fig. 13b. When the main bamboo fiber direction was longitudinal as the long side of specimens, the G2 specimens can be defined as $G2_l$, whilst, the transverse specimens can be defined as $G2_t$. The physical details of all specimens can be illustrated in Table 6.

Table 7. Testing matrix.

	Name	Characteristic	Number (fungal observations)	Number (mechanical tests)
Thick-strip	$G1_n$	Non	12	12
	$G1_m$	Medium	12	12
	$G1_d$	Deep	12	12
Thin-strip	$G2_l$	Longitudinal	12	12
	$G2_t$	Transverse	12	12

Before consequent fungal attacks, all oven-dry specimens were sterilized at 121 °C for 27 mins, under the same moisture content environment. From the controlled group without fungal attack, the average moisture content was 3.29% (SD = 0.08) for $G1_n$, 3.15% (SD = 0.36) for $G1_m$, 2.73% (SD = 0.26) for $G1_d$, 3.63% (SD = 0.37) for $G2_l$, and 3.56% (SD = 0.41) for $G2_t$. Due to the bio clean requirement of the experiments, the sterile program was taken as the conserving program to control the moisture contents of all the specimens.

The testing matrix is shown in Table 7. A total of 120 specimens were applied for fungal observation and mechanical tests. Each case involved 24 specimens, 12 of which were for fungal impacts, and another 12 for the compression tests. For thick-strip glubam, the compression tests were not conducted for the compression tests along the transverse orientation, since the bamboo strips are configured only in the longitudinal direction[45], which is the main direction for its application.

Preparation of potato dextrose agar medium (PDA)

According to GB/T 13942.1[46] and ASTM G21[47] standards, fungal cultures were maintained on potato dextrose agar medium (PDA; Solarbio, China). To craft the medium, 23 g of potato dextrose agar were combined with 500 ml of ultra-distilled water, and this mixture was subjected to controlled heat until complete dissolution was achieved. The solution underwent sterilization at a temperature of 115 °C for a duration of 20 min, ensuring the elimination of any potential contaminants. A graphical representation of the procedure is depicted in Fig. 14a.

Preparation of river sand sawdust substrate

The cultivation container employed for this purpose was a medical-grade stainless steel disinfection box, characterized by dimensions of 30 cm in length, 20 cm in width, and 5 cm in

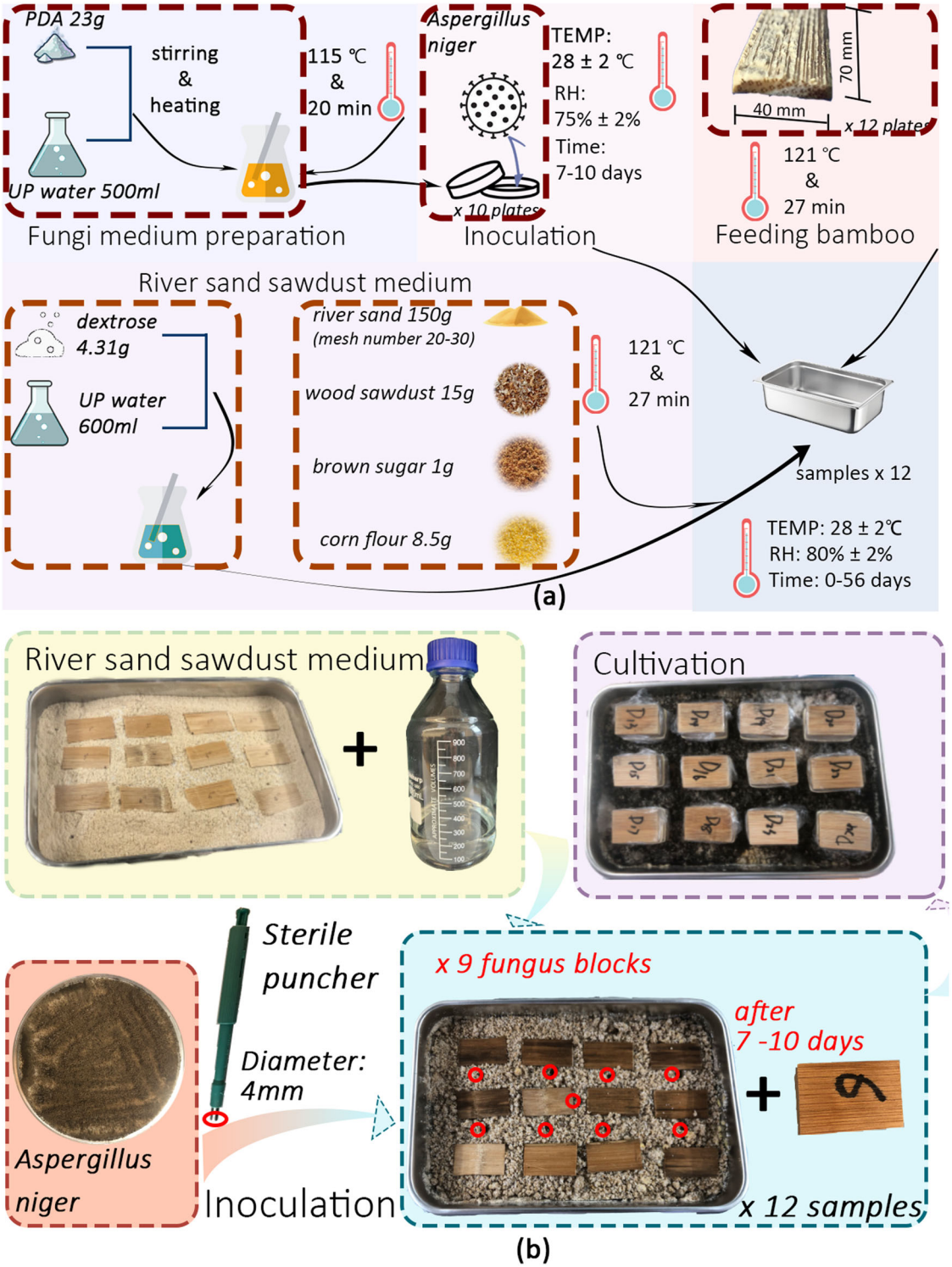

Fig. 14 Preparation of fungal attack tests. a Details of medium preparation. **b** Details of cultivation. TEMP means temperature, and RH means relative humidity.

depth. Adhering to the guidelines set forth by GB/T 13942.1, the river sand sawdust substrate was composed of two distinct components. One component of the river sand sawdust substrate was constituted by 150 g clean river sand with 20 to 30 as the mesh number, 15 g wood sawdust, 1 g brown sugar, and 8.5 g corn flour[46]. The other component of the substrate was made up of a solution of dextrose (4.31 g) and 600 ml of ultra-distilled water. A total of 12 feeder bamboo strips were, measuring 50 mm in length, 20 mm in width, and 2 mm in thickness for each culture glubam specimen. These bamboo strips were positioned atop the surface of the substrate. Both constituent parts of the substrate underwent sterilization at a temperature of 121 °C for 27 mins, which can be illustrated in Fig. 14a.

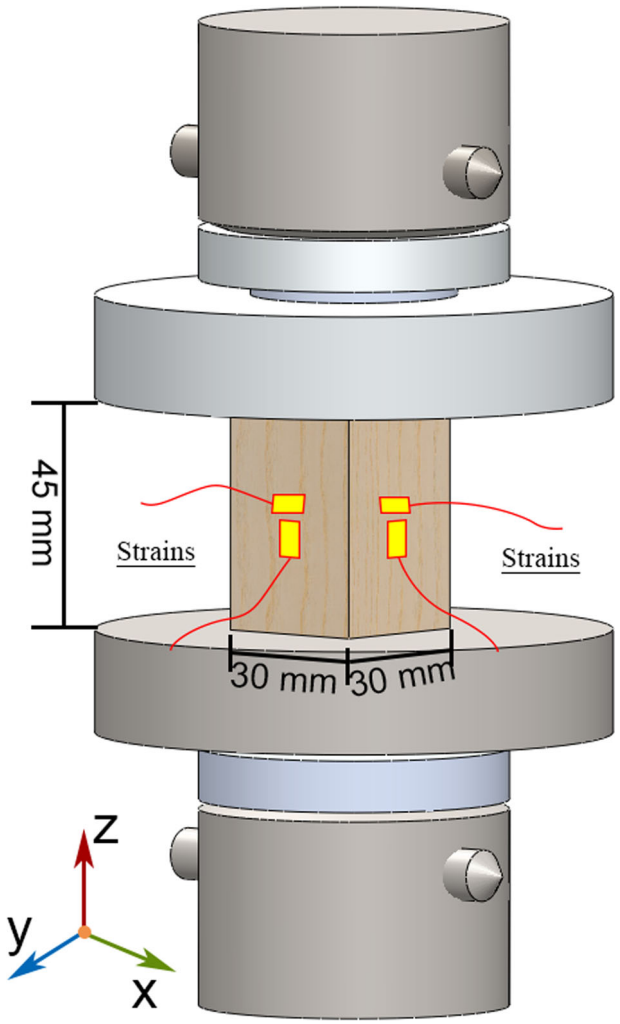

Fig. 15 Setup details for compression tests. The orthometricstrain gauges on each side of specimens are showed.

Mold infection and cultivation experiment

According to the GB/T 18261[48], the choice for this study was Aspergillus niger (*A. niger*). *A. niger* was inoculated onto the potato dextrose agar (PDA) medium within a sterile environment. The cultures were cultivated in the incubator at 28 ± 2 °C, 75 ± 2 % relative humidity (RH) for 7 to 10 days[46]. The sterile puncher with a diameter of 4 mm was employed to extract 9 agar discs from the PDA medium, each hosting fungal growth. The fungus blocks were inserted into the substrate at a depth of 5 mm beneath the surface, shown in Fig. 14b. An additional 7 to 10 days were allocated for the growth phase, during which the surface of the river sand sawdust substrate and feeder strips became enshrouded with fungal growth. The sterilized glubam specimens were positioned atop the feeder bamboo strips. This marked the commencement of the cultivation phase, a process initiated upon sealing the stainless steel container. To concentrate more on the fungal incubation from the glubam panel surface, the cutting faces were encased in plastic film. Both the specimens and A. niger cultures resided within a controlled incubator, characterized by a consistent temperature of 28 ± 2 °C, 80 ± 2 % RH for 56 days. All manipulations associated with fungal infection were conducted within the confines of a product-protective horizontal laminar-flow clean bench, providing an environment of optimal sterility (Heal Force Ltd., Shanghai). The experimental assessment encompassed the study of infection duration. Six specimens were selected from each experimental case. Subdividing these into two groups, three specimens were designated for assessing fungal influences, while the remaining three were earmarked for evaluating compressive properties. These assessments were conducted following infection durations of 14, 28, 42, and 56 days, respectively. At the termination of each designated time frame, the fungal growth on the glubam surface was cleared through the application of alcohol-wet wipes.

Quasi-static compression tests

Compression tests in the z-axis (main bamboo fiber direction) were performed as shown in Fig. 15, according to ASTM D 143[49]. A universal testing machine with 100 kN capacity was employed for quasi-static compression tests. The loading was applied continuously throughout the test at the same rate of 2 mm/min to measure the compression strength. The modulus of elasticity in compression was analyzed by 2-cycle loading, all G1 and $G2_l$ specimens were loaded from 4000 N to 8000 N, whilst $G2_t$ specimens were loaded from 2000N to 4000 N, based on the ultimate compressive loads of the specimens[41]. To simplify the calculation, the specimen is assumed homogeneous, continuities, and isotropic. To collect the strain values during the compressive test, two orthogonal strains were used on each side of the specimens, which indicates that a total of 8 strain gauges recorded the data.

Fourier transforms infrared spectrometry (FTIR)

Analysis of 10 groups of glubam slices, each with dimensions of 2.00 mm thick, 7.00 mm wide, and 10.00 mm long, were carried out analyses of FTIR. A Bruker Invenio S FTIR spectrometer was used to record spectra, with a scan rate of 8 scans per minute and a resolution of 4 cm^{-1} in the wave number region between 4000 cm^{-1} to 500 cm^{-1}.

Optical Microscopy

Amongst three specimens for fungal observations from each type of glubam specimens at each period, two blocks were picked to cut along (45 mm × 30 mm × 10 mm) and perpendicular (30 mm × 30 mm × 10 mm–15 mm) to the long side direction separately. A diamond wire cutting machine (STX-202A, Shenyang Kejing Auto-instrument Co., Ltd.) was used to slice up the specimens. After drying the sections naturally, optical microscopy photographs were taken with the Nikon microscope and camera (LV150NA; Nikon) to examine the decay of the longitudinal and transverse slices.

Scanning Electron Microscopy

The control and fungi-exposed specimens were cut into 5 mm × 5 mm × 2 mm (width × length × thickness) slices from the infected surface of each case under various periods by a diamond wire cutting machine. Slices were cleaned with alcohol-wet wipes and dehydrated in a dryer at 60 °C for 30 mins. After the pretreatment, the slices were carefully mounted on SEM stubs. A Carl Zeiss SEM micrograph machine (GeminiSEM300; Germany) was used for electron microscopy observation.

Statistical analysis

Two-way analyses of variance (ANOVA) for physical and mechanical data were performed using MATLAB R2022b software. The effects of deterioration time and glubam types on properties can be determined. Differences were considered statistically significant when $p < 0.05$.

DATA AVAILABILITY

Some of all data, models, or codes that support the findings of this study are available from the corresponding author upon reasonable request.

Received: 15 April 2023; Accepted: 23 October 2023;
Published online: 29 November 2023

REFERENCES

1. Xiao, Y., Inoue, M., & Paudel, S. K. *Modern Bamboo Structures: Proceedings of the first International conference*. (Eds.) 231-246 (CRC Press, 2008).
2. Sharma, B., Gatoo, A., Bock, M., Mulligan, H. & Ramage, M. Engineered bamboo: State of the art. *P I CIVIL ENG-CIV EN* **168**, 57–67 (2015).
3. Food and Agriculture Organization of the United Nations. Global Forest Resources Assessment 2020: Main report. (2020).
4. Xiao, Y., Zhou, Q. & Shan, B. Design and Construction of Modern Bamboo Bridges. *J. Bridge Eng.* **15**, 533–541 (2010).
5. Xiao, Y., Yang, R. Z. & Shan, B. Production, environmental impact and mechanical properties of glubam. *Constr. Build Mater.* **44**, 765–773 (2013).
6. Xiao, Y. Engineered Bamboo. In *Nonconventional and Vernacular Construction Materials*. 433–452 (Woodhead, 2016).
7. Xiao, Y., Shan, B., Chen, G., Zhou, Q. & She, L. Y. Development of a new type Glulam-GluBam. *Modern bamboo structures, ICBS-2007* 41–47 (2008)
8. Xiao, Y., Li, L. & Yang, R. Z. Long-term loading behavior of a full-scale glubam bridge model. *J. Bridge Eng.* **19**, 04014027 (2014).
9. Xiao, Y. *Engineered Bamboo Structures*. (CRC press, 2022).
10. Zhang, J. et al. Inhibition mechanism and antibacterial activity of natural antibacterial agent citral on bamboo mould and its anti-mildew effect on bamboo. *Royal Soc. Open Sci.* **8**, (2021).
11. Zhang, J. et al. Antimildew treatment and control effect of citral on bamboo. *Int J. Polym. Sci.* **2021**, 1–10 (2021).
12. Huang, X. D., Hse, C. Y. & Shupe, T. F. Study on the Mould-resistant properties of moso bamboo treated with high pressure and amylase. *Bioresources* **9**, 497–509 (2014).
13. Kim, J. J. et al. Fungi associated with bamboo and their decay capabilities. *Holzforschung* **65**, 271–275 (2011).
14. Yan, J. et al. Antifungal effect of seven essential oils on bamboo. *Adv. Compos Hybrid. Mater.* **4**, 552–561 (2021).
15. Schmidt, O., Wei, D. S., Tang, T. K. H. & Liese, W. Bamboo and fungi. *J. Bamboo Rattan* **12**, 1–14 (2013).
16. Xu, G., Wang, L., Liu, J. & Wu, J. FTIR and XPS analysis of the changes in bamboo chemical structure decayed by white-rot and brown-rot fungi. *Appl. Surf. Sci.* **280**, 799–805 (2013).
17. Meng, F. et al. Improvement of the water repellency, dimensional stability, and biological resistance of bamboo-based fiber reinforced composites. *Polym. Compos.* **40**, 506–513 (2019).
18. Kumar, A., Ryparová, P., Kasal, B., Adamopoulos, S. & Hajek, P. Resistance of bamboo scrimber against white-rot and brown-rot fungi. *Wood Mater. Sci. Eng.* **15**, 57–63 (2020).
19. Liu, X. et al. Improving mechanical toughness and mold resistance of bamboo/high-density polyethylene composites by pretreatment with the fungus Trametes versicolor. *Polym. Compos* **43**, 1438–1447 (2022).
20. Feng, J. et al. Effects of fungal decay on properties of mechanical, chemical, and water absorption of wood plastic composites. *J. Appl Polym. Sci.* **138**, 50022 (2021).
21. Crawford, B. et al. Effect of fungal deterioration on physical and mechanical properties of hemp and flax natural fiber composites. *Materials* **10**, 1252 (2017).
22. Clemons, M. C. & Ibach, E. R. Laboratory tests on fungal resistance of wood filled polyethylene composites. *Annu. Tech. Conf.* **2**, 2219–2223 (2002).
23. Feng, J., Zhang, H., He, H., Huang, X. & Shi, Q. Effects of fungicides on mold resistance and mechanical properties of wood and bamboo flour/high-density polyethylene composites. *Bioresources* **11**, 4069–4085 (2016).
24. Sun, F., Bao, B., Ma, L., Chen, A. & Duan, X. Mould-resistance of bamboo treated with the compound of chitosan-copper complex and organic fungicides. *J. Wood Sci.* **58**, 51–56 (2012).
25. Li, J. et al. Durable, self-cleaning and superhydrophobic bamboo timber surfaces based on TiO2 films combined with fluoroalkylsilane. *Ceram. Int.* **42**, 9621–9629 (2016).
26. Bobadilha, G. S. et al. Effect of exterior wood coatings on the durability of cross-laminated timber against mold and decay fungi. *Bioresources* **15**, 8420–8433 (2020).
27. Wang, D. et al. Bamboo surface coated with polymethylsilsesquioxane/Cu-containing nanoparticles (PMS/CuNP) xerogel for superhydrophobic and anti-mildew performance. *J. Wood Sci.* **66**, 1–8 (2020).
28. Yuan, Z. et al. Effects of one-step hot oil treatment on the physical, mechanical, and surface properties of bamboo scrimber. *Molecules* **25**, 4488 (2020).
29. Tang, T. et al. Synergistic effects of tung oil and heat treatment on physico-chemical properties of bamboo materials. *Sci. Rep.* **9**, 12824 (2019).
30. Hao, X. et al. The effect of oil heat treatment on biological, mechanical and physical properties of bamboo. *J. Wood Sci.* **67**, 1–14 (2021).
31. Kwaśniewska-Sip, P., Bartkowiak, M., Cofta, G. & Nowak, P. B. Resistance of Scots pine (Pinus sylvestris L.) after treatment with caffeine and thermal modification against Aspergillus niger. *Bioresources* **14**, 1890–1898 (2019).
32. Maria Silva Brito, F., Benigno Paes, J., Tarcísio da Silva Oliveira, J., Donária Chaves Arantes, M. & Dudecki, L. Chemical characterization and biological resistance of thermally treated bamboo. *Constr. Build Mater.* **262**, 120033 (2020).
33. Bellon, K. R. et al. Behavior of thermally modified wood to biodeterioration by xylophage fungi. *Cerne* **26**, 331–340 (2020).
34. Yang, K., Li, X., Wu, Y. & Zheng, X. A simple, effective and inhibitor-free thermal treatment for enhancing mold-proof property of bamboo scrimber. *Eur. J. Wood Wood Prod.* **79**, 1049–1055 (2021).
35. Ogutuga, S. O., Olasupo, O. O., Adebayo, S. O. & Ojo, A. R. Effect of heat treatment on the durability of laminated bamboo against brown rot fungus (Sclerotium Rolfsii Sacc) Attack. *JWHSD* **3**, 49–58 (2015).
36. Shangguan, W., Gong, Y., Zhao, R. & Ren, H. Effects of heat treatment on the properties of bamboo scrimber. *J. Wood Sci.* **62**, 383–391 (2016).
37. Li, Q., Wen-Ji, Y. & Yang-Lun, Y. Research on properties of reconstituted bamboo lumber made by thermo-treated bamboo bundle curtains. *Prod. J.* **62**, 545–550 (2012).
38. Brito, F. M. S. et al. Physico-mechanical characterization of heat-treated glued laminated bamboo. *Constr. Build Mater.* **190**, 719–727 (2018).
39. Schmidt, G., Stute, T., Lenz, M. T., Melcher, E. & Ressel, J. B. Fungal deterioration of a novel scrimber composite made from industrially heat treated African highland bamboo. *Ind. Crops Prod.* **147**, 112225 (2020).
40. Standards of the People's Republic of China. GB/T 1935-2009 Method of testing in compressive strength parallel to grain of wood. (2009).
41. Standards of the People's Republic of China. GB/T 1943-2009 Method for determination of the modulus of elasticity in compression perpendicular to grain of wood.
42. Omemu, A. M., Akpan, I., Bankole, M. O. & Teniola, O. D. Hydrolysis of raw tuber starches by amylase of Aspergillus niger AM07 isolated from the soil. *Afr. J. Biotechnol.* **4**, 19–25 (2005).
43. Hrmová, M., Biely, P. & Vršanská, M. Cellulose-and xylan-degrading enzymes of Aspergillus terreus and Aspergillus niger. *Enzym. Microb. Technol.* **11**, 610–616 (1989).
44. Al-Rukaibawi, L. S., Omairey, S. L. & Károlyi, G. A numerical anatomy-based modelling of bamboo microstructure. *Constr. Build Mater.* **308**, 125036 (2021).
45. Li, Z., He, X. Z., Cai, Z. M., Wang, R. & Xiao, Y. Mechanical properties of engineered bamboo boards for glubam structures. *J. Mater. Civ. Eng.* **33**, 04021058 (2021).
46. Standards of the People's Republic of China. GB/T 13942.1-2009 Durability of wood- Part 1: Method for laboratory test of natural decay resistance. (2015).
47. Materials, I. et al. ASTM G21-15 Standard Practice for Determining Resistance of Synthetic Polymeric Materials to Fungi. 19–24 Preprint at (2020). https://doi.org/10.1520/G0021-15.2
48. Standards of the People's Republic of China. GB/T 18261-2013 Test method for anti-mildew agents in controlling wood mould and stain fungi.
49. ASTM D143. Standard Test Methods for Small Clear Specimens of Timber (2022). https://www.astm.org/d0143-22.html.

ACKNOWLEDGEMENTS

The research reported in this paper has been conducted under the support of the Zhejiang University Presidential Fund (2021XZZX040), and the UAD Center (KH20203315C), the research specimens were prepared at the ZJU-Ninghai Center for Bio-based Materials and Carbon Neutral Development.

AUTHOR CONTRIBUTIONS

C.C. conceived and designed the overall study and helped to analyze the results and draft the manuscript. S.Z. carried on the fungal experimental work. Y.K. carried on the mechanical experimental work. T.J. helped with the fungal experimental work. W.H. supported the fungal experimental work and reviewed the paper. Y.H. helped with the fungal experimental work. D.Z. supported the fungal experimental work and reviewed the paper. Y.X. conceived, designed, and coordinated the overall study, helped to analyze the results, and revised the paper. All authors read and approved the final manuscript.

COMPETING INTERESTS

The authors declare no competing interests.

ADDITIONAL INFORMATION

Correspondence and requests for materials should be addressed to Y. Xiao.

Reprints and permission information is available at http://www.nature.com/reprints

Publisher's note Springer Nature remains neutral with regard to jurisdictional claims in published maps and institutional affiliations.